Engineering Transactions, **67**(3): 411–427, 2019, doi: 10.24423/EngTrans.945.20190509
Polish Academy of Sciences • Institute of Fundamental Technological Research (IPPT PAN)
Université de Lorraine • Poznan University of Technology

Research Paper

Performance Evaluation and Frequency Response Analysis of a Two Stage Two Spool Electrohydraulic Servovalve with a Linearized Model

Nitesh MONDAL[1)*], Biswanath DATTA[2)]

[1)] *Department of Mechanical Engineering*
Jadavpur University
Kolkata, India
*Corresponding Author e-mail: niteshju@yahoo.com

[2)] *Indian Institutes of Engineering Science and Technology*
Shibpur, Howrah, India

This article focuses on the performance study and frequency response analysis with the state space model of a linearized two stage two spool non-conventional electrohydraulic servovalve from a set of nonlinear state equations. The performance of this valve depends on many valve geometries and fluid parameters. This non-conventional electrohydraulic servovalve is controlled by a pressure controlled pilot, which generates a differential pressure between the upper and lower chambers of two spools. This differential pressure acts as the feedback element, thereby reducing the requirement for a feedback wire. In this paper, the dynamic behaviour and state-space model of the valve is established with the aid of linearized mathematical equations and the coefficients of the equations directly depend on the valves parameters, fluid properties and flow properties. The dynamic performance of this valve and the frequency response are analysed with the help of MATLAB/Simulink.

Key words: electrohydraulic servovalve; two-stage-two-spool; pressure feedback; state-space model; frequency response.

1. Introduction

Electrohydraulic servovalves are electrically operated valves which regulate the flow of hydraulic fluid to the connected actuator, which results in controlled acceleration, velocity and displacement of the actuator. This hydraulic component was popularised at the end of the last century primarily owing to the properties such as high power-to-weight ratio, ease of control and superior performance. They are used in the precision flow and position control applications such as in computer numerical controlled (CNC) machine tools, in aircraft con-

trol surfaces and all kinds of off-highway applications [1–5]. The existence of a feedback element in such a two stage servovalve is customary, however an alternate two stage servovalve design comprising two spools is rather unique since it acts on the same principles without the aid of a feedback element. This servovalve design simplifies the system assembly and provides higher degree of adjustment along with superior safety [6]. Despite such benefits literature suggests that much research is not available on this particular two stage servovalve design. Most of the available research is directed towards the improvement of a single spool design, like Kim and Tsao [7] analysed the dynamic sensitivity of the two stage single spool valve by a linearized model. Lin and Akers [8] studied the dynamics of a flapper nozzle, differential pressure and the frequency response of a flapper nozzle assembly. They concluded that oil temperature and small tolerance in the components have no significant influence on the valve performance. Bang *et al.* [9] represented a model of two stage electrohydraulic servovalve by using a stack type piezoelectric element and demonstrated that the flapper movement varies linearly with the differential voltage and the flow rate of the valve varies with the variation of supply pressure [10]. Yuan and Jee [11] modelled an energy saving two stage twin spool servovalve design used in mobile hydraulic platforms and concluded that the system can accumulate superfluous energy even with a load sensing pump. Yoshida and Miyakaya [12] discuss about the frequency response analysis of a proportional control valve and studied the effect of the parameters on the frequency features.

There remains a necessity for analysing the static and dynamic performance characteristics of these valves in order to access their capability in comparison with the conventional two stage servovalves. These performance characteristics not only help the designer to improve the valve design as required, but equip the end user with the knowledge required to access the utility of the valve in a particular system. In order to determine these performance characteristics, the knowledge of a transfer function of the system is a prerequisite. However, the transfer function may not be available for all practical situations. Hence, the necessity of a frequency response analysis becomes significant.

Literature on the subject suggests that a detailed study of split spool type EHSV with pressure control feedback is a necessity for contemporary designers, since it is likely to reduce the servomotor cost significantly. The motivation behind the proposed work is to establish an unbiased mathematical model for the split spool type electrohydraulic servomotor with pressure feedback, taking into account the non-linear effects of axial flow force and the effect of fluid compressibility. In this study, the linearized mathematical model of such a two stage two spool servovalve in the state space form is used to attain the frequency response characteristics of the valve and analyse the same in order to access its performance.

2. Operation

The schematic view of a two stage two spool pilot operated electrohydraulic servovalve is shown in Fig. 1. It consists of two stages, namely the flapper nozzle stage or pilot stage followed by the Boost stage which comprises two spools instead of one.

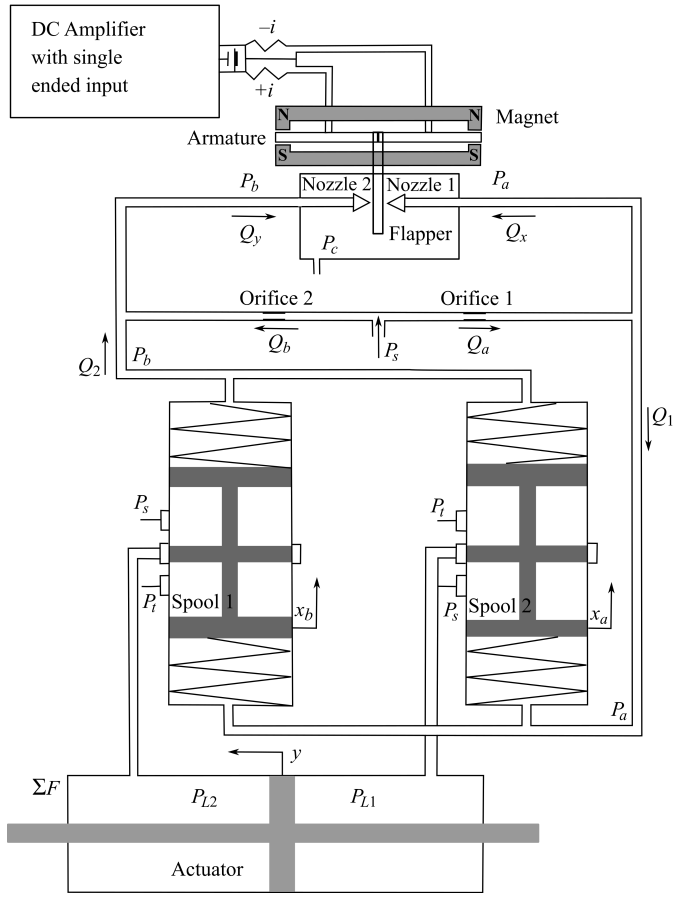

Fig. 1. Schematic of two stage two spools electrohydraulic servovalve.

The input to the two-spool two-stage electrohydraulic servovalve is typically a current or a differential current on the electromagnetic torque motor which polarizes the armature and induces a small angular rotation counter clockwise (clockwise). As a result of this rotation, the flapper moves right (left) linearly with the nozzle right (left). This movement reduces the flapper – nozzle distance for the right nozzle and increases (decreases) it for the left nozzle which in turn increases the pressure in the right-hand pressure chamber and decreases (increases) it in the left one, thus developing a differential pressure between two

chambers associated with the two ends of the spool. Thus a force imbalance is created across both ends of spool 1 and spool 2 respectively, which are connected to each other at both ends. As a result, both the spools move upward until the pressure difference is nullified and hence reaches the steady state condition. Now, if the input current is turned off, the flapper goes back to its initial position. Conventionally, in such a situation the feedback wire helps to move the spool to its initial position. However, in our case no such wire has been used. Instead, the pressure which is built up on the upper chamber of the spools and the lowering of pressure in the lower chamber of spools due to flapper movement to its initial position, leads to the formation of a reverse differential pressure. This reverse differential pressure acts as a mechanical feedback (known as pressure feedback) which causes the spools to go back to their initial positions.

Table 1. Parameters used for mathematical model of the system.

Notation	Parameter	Notation	Parameter
a_n	nozzle area	P_L	load pressure
a_o	orifice area	P_{L1}, P_{L2}	actuator chamber pressure at right and left side
a_s	cross section area of spool	P_s	supply pressure
A_P	cross section area of actuator	Q_{L1}	flow from spool 1 work port to actuator right chamber
i^*	input current of the system	Q_{L2}	flow from left chamber of actuator to spool 2
K_m	torque motor stiffness	V_l	volume of the actuator chamber
K_t	torque motor gain	x_f	flapper displacement
M	mass of piston and load together	x_a, x_b	spool displacement of spool 1 and spool 2
P_c	chamber pressure	y	actuator position displacement
P_a, P_b	pressure in right and left conduit	$\dot{y}$, $\ddot{y}$	actuator velocity and acceleration
P_{ao}, P_{bo}	initial back pressure in the right and left nozzle	θ	angle of rotation of the flapper

3. Servovalve dynamics

3.1. Dynamics of the pilot stage

At the null position of the armature, there is no deflection in it because a symmetrical air gap is considered between the armature and magnet. The applied current through the torque motor coils is the cause of polarization of the armature ends. Hence, a torque is produced on the armature which makes it move. To calculate this torque a linear expression is used as [2, 13],

$$T_d = K_t i^* + K_m \theta. \tag{3.1}$$

K_t and K_m are known as torque motor gain and torque motor stiffness, respectively, and represent as

$$K_t = \frac{2aN\phi}{g} \qquad \text{and} \qquad K_m = \frac{4a^2\phi^2}{g\mu_0 A_g},$$

where a is the half of the armature rod length, N is the number of turns of the coil, ϕ is magnetic flux, g is the initial air gap between armature and permanent magnet, μ_0 is the absolute permeability of air, and A_g is the pole face area.

Asymmetric flow forces are created on the two sides of the flapper and this flow forces developed a resisting torque T_f on the flapper and can be formulated as follows [2]:

- force due to right nozzle:

$$F_x = P_a a_n + 4\pi C_{qn}^2 \left(x_{fo}^2 - 2x_{fo}x_f\right)(P_a - P_c), \tag{3.2}$$

- force due to left nozzle:

$$F_y = P_b a_n + 4\pi C_{qn}^2 \left(x_{fo}^2 + 2x_{fo}x_f\right)(P_b - P_c). \tag{3.3}$$

Therefore, the developed resisting torque T_f on the flapper due to this asymmetric flow forces is:

$$T_f = (F_x - F_y)r = (P_a - P_b)a_n r + 4\pi C_{qn}^2 x_{fo}^2 (P_a - P_b)r - 8\pi C_{qn}^2 x_{fo}(P_a + P_b)r^2\theta. \tag{3.4}$$

Taking the value of $P_c = 0$ as atmospheric pressure.

So the net torque acting on the torque motor is:

$$T_d - T_f = J_a\ddot{\theta} + B_a\dot{\theta} + K_a\theta. \tag{3.5}$$

After putting the value of T_d and T_f the above equation becomes

$$K_t i^* = (K_a - K_m)\theta + (P_a - P_b)a_n r + 4\pi C_{qn}^2 x_{fo}^2 (P_a - P_b)r - 8\pi C_{qn}^2 x_{fo}(P_a + P_b)r^2\theta + J_a\ddot{\theta} + B_a\dot{\theta}. \tag{3.6}$$

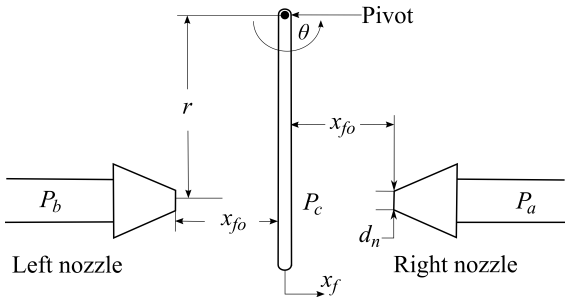

FIG. 2. Schematic of flapper nozzle.

3.2. Dynamics of the boost stage

A dynamics equation is needed to describe the forces acting on the assumed critically centred spool. There are four forces at play on both spools viz. the differential pressure force acting at the two ends of the spools, spring force acting due to the two centring springs, viscous damping force and axial flow force. The dynamic equation of the spool 1 and spool 2 can be represented by

$$m_s\ddot{x}_a = (P_a - P_b)a_s - 2K_s x_a - B_s\dot{x}_a - f_{xa}, \tag{3.7}$$

$$m_s\ddot{x}_b = (P_a - P_b)a_s - 2K_s x_b - B_s\dot{x}_b - f_{xb}. \tag{3.8}$$

The axial flow forces are determined by the Reynold's transport theorem [13–15], where the general form of this theorem to evaluate the net force induced due to the flow f is given by

$$f = \int\limits_{CS} \rho\overline{v}\left(\overline{v}\,\mathrm{d}\overline{A}\right) + \frac{\mathrm{d}}{\mathrm{d}t}\int\limits_{CV}\rho\overline{v}\,\mathrm{d}V + \frac{\mathrm{d}^2}{\mathrm{d}t^2}\int\limits_{CV}\rho\,\mathrm{d}V. \tag{3.9}$$

The first term of Eq. (3.9) represents the net rate of flux of momentum from control volume through control surface, second term denotes the local rate of change of momentum within the control volume and the third term is related to the material rate of change of momentum due to moving boundary. Now, the final form of an axial flow force on the spool 1 and spool 2 are given by

$$f_{xa} = \frac{C_q^2 w x_a\cos\alpha}{C_c}(P_s - P_{L1}) + \rho C_q w\sqrt{\frac{2}{\rho}}\left[(P_s - P_{L1})\dot{x}_a - \frac{1}{2}\frac{x_a}{\sqrt{(P_s - P_{L1})}}\dot{P}_{L1}\right]L_{S1} + m_{cV}\ddot{x}_a, \tag{3.10}$$

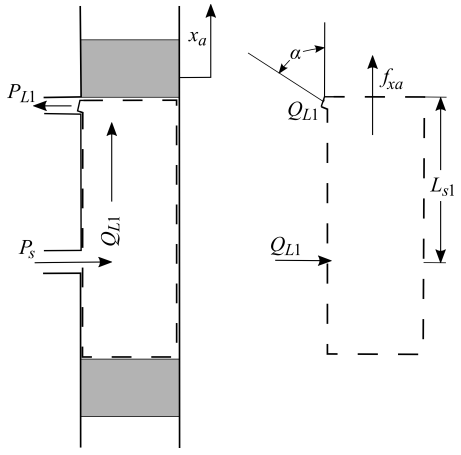

FIG. 3. Control volume analysis for flow force.

$$f_{xb} = \frac{C_q^2 w x_b \cos\alpha}{C_c}(P_s - P_{L2}) + \rho C_q w \sqrt{\frac{2}{\rho}} \left[(P_s - P_{L2})\dot{x}_b - \frac{1}{2} \frac{x_a}{\sqrt{(P_s - P_{L2})}} \dot{P}_{L2} \right] L_{D2} + m_{cV} \ddot{x}_b. \tag{3.11}$$

3.3. Dynamics of chamber pressure

The pilot pressure P_a, P_b are needed as input to the both pilot stage Eq. (3.6) and the boost stage Eqs (3.7) and (3.8) dynamics. Considering the effect of fluid compressibility, the chamber pressure P_a and P_b have been determined by the basic hydraulic compressibility equations as follows:

- for right nozzle:

$$Q_1 = Q_a - Q_x = a_s \dot{x}_a + a_s \dot{x}_b + \frac{V_a}{\beta} \dot{P}_a, \tag{3.12}$$

- for left nozzle:

$$Q_2 = Q_y - Q_b = a_s \dot{x}_a + a_s \dot{x}_b - \frac{V_b}{\beta} \dot{P}_b. \tag{3.13}$$

3.4. Dynamics of the load stage

Considering the valve is critical-centred, the effect of fluid compressibility and the piston position is at the middle of the load actuator, the relations of flow from the valve to the actuator can be obtained from the principle of continuity as follows

$$Q_{L1} = C_q w x_a \sqrt{\frac{1}{\rho}(P_s - P_L)} = A_P \dot{y} + \frac{V_l}{\beta} \dot{P}_L \tag{3.14}$$

and

$$Q_{L2} = C_q w x_b \sqrt{\frac{1}{\rho}(P_s - P_L)} = A_P \dot{y} + \frac{V_l}{\beta} \dot{P}_L, \tag{3.15}$$

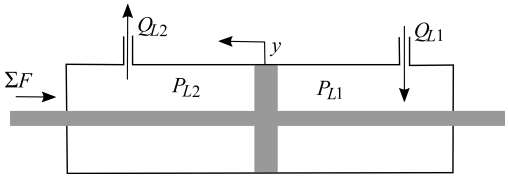

FIG. 4. Load stage dynamics.

where A_P is the cross sectional area of the actuating piston and V_l is the volume of the load or actuating chamber of both side:

$$P_L A_P = m\ddot{y} + B\dot{y} + Ky + F_c(\operatorname{Sgn}\dot{y}). \tag{3.16}$$

In the above equation the left side force is the pressure force or load force on the load actuator, the first term of the right side indicates the inertia force, the second term is for the viscous force, the third term comes due to the stiffness of the piston rod and the last term indicates the striction force.

3.5. Model of the flow equation

We assume that the spool port of the valve is rectangular in its geometry. When the spool moves, flow is either metered into or out of the valve through this rectangular orifice. The movement of a spool upward x_a, $x_b > 0$, as shown in Fig. 1, creates a flow which can be represented by

$$Q_{L1} = C_q w x_a \sqrt{\frac{2}{\rho}(P_s - P_{L1})}, \tag{3.17}$$

$$Q_{L1} = C_q w x_b \sqrt{\frac{2}{\rho}(P_{L2} - P_t)}. \tag{3.18}$$

4. Linearized servovalve model

The non-linear nature of the electrohydraulic system is quite evident from the mathematical model of the two stage two spool electrohydraulic servovalve. However, for ease of implementation and analysis, the present investigation deals with a linearized model of the system. This simplified system model is formed by combining various system parameters as single system coefficients, so that the servovalve performance can be improved by the optimum choice of these coefficients. The linearized model is derived from the Eqs (3.6)–(3.8), (3.12), and (3.13) with respect to an equilibrium state which is defined as the zero input state ($i^* = 0$). The complete linearized model can be represented as

$$\Delta\ddot{\theta} = -C_1\Delta\theta - C_2\Delta\dot{\theta} - C_3\Delta P_a + C_5\Delta i^*, \tag{4.1}$$

$$\Delta\dot{P}_a = C_6\Delta\theta - C_7\Delta P_a - C_8\Delta\dot{x}_a - C_9\Delta\dot{x}_b, \tag{4.2}$$

$$\Delta\dot{P}_b = -C_{10}\Delta\theta - C_{11}\Delta P_a + C_{12}\Delta\dot{x}_a + C_{13}\Delta\dot{x}_b, \tag{4.3}$$

$$\Delta\ddot{x}_a = C_{14}\Delta P_a - C_{15}\Delta P_b - C_{16}\Delta x_a - C_{17}\Delta\dot{x}_a, \tag{4.4}$$

$$\Delta\ddot{x}_b = C_{18}\Delta P_a - C_{19}\Delta P_b - C_{20}\Delta x_b - C_{21}\Delta\dot{x}_b, \tag{4.5}$$

where

$$C_1 = \frac{\left\{K_a - K_m - 8\pi C_{qn}^2 x_{fo}(P_{ao} + P_{bo})\, r^2\right\}}{J_a}, \tag{4.6}$$

$$C_2 = \frac{B_a}{J_a}, \tag{4.7}$$

$$C_3 = \frac{\left(a_n r + 4\pi C_{qn}^2 x_{fo}^2 r - 8\pi C_{qn}^2 x_{fo} r^2 \theta_o\right)}{J_a}, \tag{4.8}$$

$$C_4 = \frac{\left(a_n r + 4\pi C_{qn}^2 x_{fo}^2 r + 8\pi C_{qn}^2 x_{fo} r^2 \theta_o\right)}{J_a}, \tag{4.9}$$

$$C_5 = \frac{K_t}{J_a}, \tag{4.10}$$

$$C_6 = \frac{\beta}{V_a}\left(C_{qn}\pi d_n r\sqrt{\frac{2}{\rho}P_{ao}}\right), \tag{4.11}$$

$$C_7 = \frac{\beta}{V_a}\left[\frac{C_{qo}a_o}{\sqrt{2\rho(P_s - P_{ao})}} + \frac{C_{qn}\pi d_n(x_{fo} - r\theta_o)}{\sqrt{2\rho P_{ao}}}\right], \tag{4.12}$$

$$C_8 = C_9 = \frac{\beta}{V_a}a_s, \tag{4.13}$$

$$C_{10} = \frac{\beta}{V_b}\left(C_{qn}\pi d_n r\sqrt{\frac{2}{\rho}P_{bo}}\right), \tag{4.14}$$

$$C_{11} = \frac{\beta}{V_b}\left[\frac{C_{qo}a_o}{\sqrt{2\rho(P_s - P_{bo})}} + \frac{C_{qn}\pi d_n(x_{fo} + r\theta_o)}{\sqrt{2\rho P_{bo}}}\right], \tag{4.15}$$

$$C_{12} = C_{13} = \frac{\beta}{V_b}a_s, \tag{4.16}$$

$$C_{14} = C_{15} = C_{18} = C_{19} = \frac{a_s}{m_s + m_{cV}}, \tag{4.17}$$

$$C_{16} = C_{20} = \frac{1}{m_s + m_{cV}}\left[\frac{C_q^2}{C_c}\cos\theta_f w(P_s - P_{Lo}) + 2K_S\right], \tag{4.18}$$

$$C_{17} = C_{21} = \frac{1}{m_s + m_{cV}}\left[C_q w L_P\sqrt{\rho(P_s - P_{Lo})} + B_S\right]. \tag{4.19}$$

5. Characteristics of two-stage two-spool electrohydraulic servovalve at varied supply pressures

The simulation model for two spool split type EHSV with hydraulic servomotor serving as the load is developed using linearized model Eqs (4.1) through (4.5) in MATLAB/Simulink. The solver for the Simulation model is chosen as the variable step type ode 45 solver used for solving non-stiff differential equations with relative tolerance of 1e–03. A steady-state load flow has been considered

Table 2. The following parameters were used in the modeling of this paper.

Parameter	Notation	Value (unit)
Initial air gap between armature & permanent magnet	g	300.00e–06 m
Half of the armature rod length	a	16.00e–03 m
Absolute permeability of air	μ_o	12.5663e–07 H/m
Pole face area	A_g	10.000e–06 m^2
Magnetic flux	ϕ	9.300e–06 Wb
Number of turns of coil	N	4400
Flexure tube stiffness	K_a	27.1562e03 N/m
Armature viscous damping coefficient	B_a	1.21037e–03
Polar moment of inertia of spool	J_a	3.05352e–07 $kg \cdot m^2$
Flapper length	r	1.560e–02 m
Nozzle diameter	d_n	200.000e–06 m
Flapper nozzle discharge coefficient	C_{qn}	0.6200
Initial gap between flapper & nozzle	x_{fo}	65.000e–06 m
Orifice discharge coefficient	C_q	0.6200
Supply orifice diameter	d_o	40.000e–06 m
Volume of chamber	V_a, V_b	152.958e–09 m^3
Density of working fluid	P	870 kg/m^3
Bulk modulus of working fluid	β	1.380e09 Pa
Spool diameter	d_s	4.5580e–03 m
Spool mass	m_s	2.2000e–03 kg
Hydraulic oil mass in spool valve	m_{cV}	1.8120e–04 kg
Spool spring stiffness	K_s	300 N/m
Damping coefficient of spool	B_s	0.1920
Coefficient of contraction	C_c	0.625
Damping length	L_{s1}, L_{D2}	7.000e–03 m
Jet angle of fluid at spool orifice	α	1.2043 rad
Area of gradient of spool valve	w	2.9000e–03 m

for a rated current of 3 mA, spring stiffness 300 N/m^2, damping length 7e–03 m and load end mass of 1000 kg at three different supply pressures. Several standard values are considered for most of the user defined servovalve parameters as provided in Table 2.

Figure 5a shows the rotation of flapper due to the polarization of the armature with 3 mA current. It can be noted from the figure that the rotation of the flapper remains the same for different supply pressures. Hence, it is safe to conclude that the rotation of flapper depends on the degree of polarization of the armature not on the supply pressure.

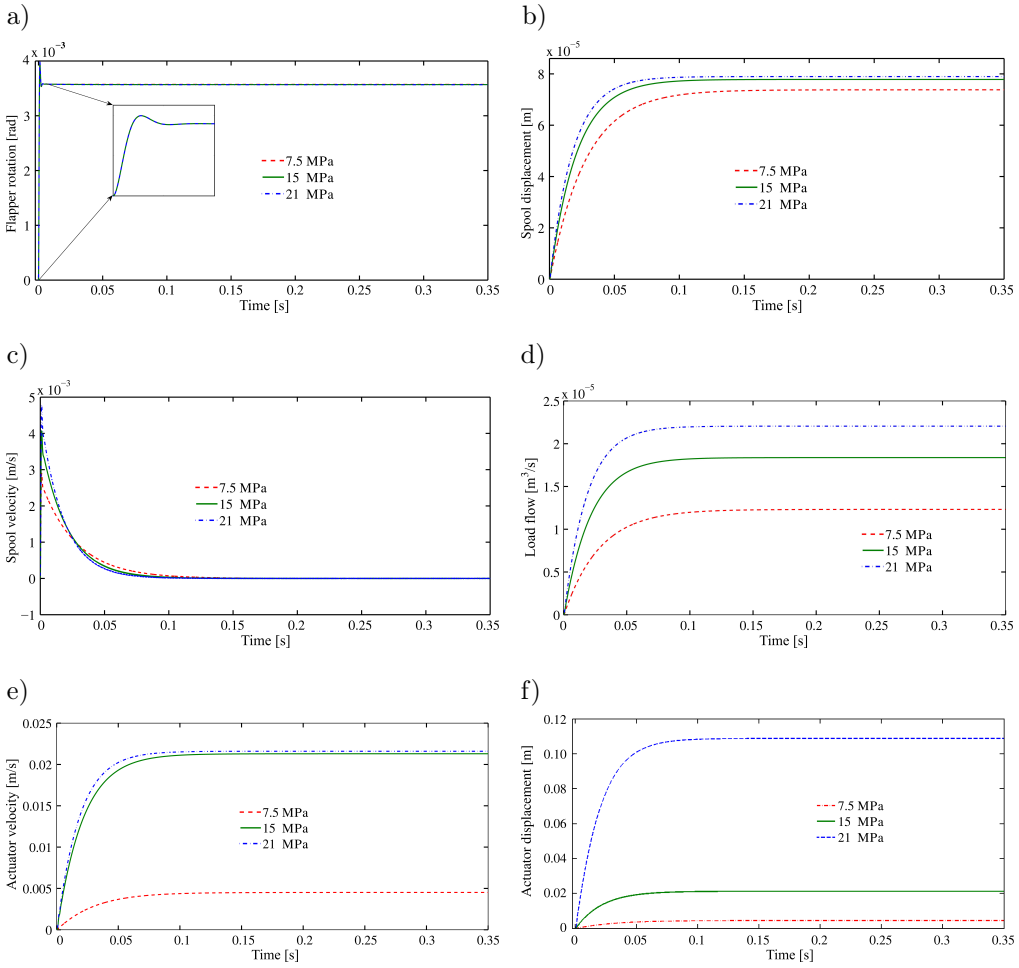

FIG. 5. Unit step response of the system for different supply pressure.

The spool displacement of the two identical spools has been shown in Fig. 5b. The spool displacement has a significant influence on the supply pressure. The

displacement of the spool increases with an increase in supply pressure owing to the increase in the chamber pressure at the spool end.

Figure 5c displays the effect of variation of supply pressure on the spool velocity. The peaks in velocity during the initial phase may be attributed to the sudden rise in flapper rotation as shown in Fig. 5a which in turn increases the pressure on the spool end and sets the spool in motion. The flapper rotation settles down to its steady state value after about 0.01 seconds as a consequence of which the pressure steadily declines on the spool end which in turn reduces the spool velocity steadily. It can be observed from the figure that as the supply pressure increases the rate of decline of the spool velocity after the initial peak response increases as well.

The steady state load flow depends on the supply pressure based on a square root relation. As the supply pressure increases, the settling time of the load flow to the steady-state reduces owing to faster spool displacement as is evident from Fig. 5d. The nature of the load flow is similar to the work done by Jie and Hongliang [10].

The velocity of an actuator is governed by the flow rate of the hydraulic fluid to the actuator from the spool which in turn depends on the supply pressure. So, we can say that the actuator velocity indirectly depends on the supply pressure. Figure 5e shows the variation of the actuator velocity with an increase in supply pressure. Similarly, Fig. 5f represents the actuator displacement with respect to the corresponding supply pressure. It is clear from the figure that the actuator displacement has a very important role, significant that the magnitude of displacement very much affected the supply pressure.

6. Frequency response analysis through state-space model of the system

The State-space model [17] of the system has been developed with the help of linearized Eqs (3.17)–(3.19) and (4.1)–(4.5). The general form of the state space model for a linear system is

$$\dot{\mathbf{x}} = \mathbf{A}\mathbf{x} + \mathbf{B}\mathbf{i}^*, \tag{6.1}$$

$$\mathbf{y} = \mathbf{C}\mathbf{x} + \mathbf{D}\mathbf{i}^*, \tag{6.2}$$

where $\mathbf{x}$ – state vector (n-vector), $\mathbf{y}$ – output vector (m-vector), $\mathbf{i}^*$ – control vector, $\mathbf{A}$ – state matrix ($n \times n$ matrix), $\mathbf{B}$ – control matrix ($n \times r$ matrix), $\mathbf{C}$ – output matrix ($m \times n$ matrix), $\mathbf{D}$ – feed-forward matrix ($m \times r$ matrix).

With the help of Eqs (3.17), (3.18) and (4.1)–(4.3) **A**, **B**, **C**, **D** are defined as

$$\mathbf{A} = \begin{bmatrix} 0 & 1 & 0 & 0 & 0 & 0 & 0 & 0 \\ -C_1 & -C_2 & -C_3 & C_4 & 0 & 0 & 0 & 0 \\ C_6 & 0 & -C_7 & 0 & 0 & -C_8 & 0 & -C_9 \\ -C_{10} & 0 & 0 & -C_{11} & 0 & C_{12} & 0 & C_{13} \\ 0 & 0 & 0 & 0 & 0 & 1 & 0 & 0 \\ 0 & 0 & C_{14} & -C_{15} & -C_{16} & -C_{17} & 0 & 0 \\ 0 & 0 & 0 & 0 & 0 & 0 & 0 & 1 \\ 0 & 0 & C_{18} & -C_{19} & 0 & 0 & -C_{20} & -C_{21} \end{bmatrix}, \quad \mathbf{B} = \begin{bmatrix} 0 \\ C_5 \\ 0 \\ 0 \\ 0 \\ 0 \\ 0 \\ 0 \end{bmatrix},$$

$$\mathbf{C} = \begin{bmatrix} 1 & 0 & 0 & 0 & 0 & 0 & 0 & 0 \\ 0 & 0 & 1 & 0 & 0 & 0 & 0 & 0 \\ 0 & 0 & 0 & 1 & 0 & 0 & 0 & 0 \\ 0 & 0 & 0 & 0 & 1 & 0 & 0 & 0 \\ 0 & 0 & 0 & 0 & 0 & 0 & 1 & 0 \end{bmatrix}, \qquad \mathbf{D} = \begin{bmatrix} 0 \\ 0 \\ 0 \\ 0 \\ 0 \end{bmatrix}.$$

Now in the system there is one input i.e. current (Δi) and five outputs

$$\mathbf{y} = \begin{bmatrix} \Delta\theta \\ \Delta P_a \\ \Delta P_b \\ \Delta x_a \\ \Delta x_b \end{bmatrix}, \qquad \mathbf{x} = \begin{bmatrix} \Delta\theta \\ \Delta\dot{\theta} \\ \Delta P_a \\ \Delta P_b \\ \Delta x_a \\ \Delta\dot{x}_a \\ \Delta x_b \\ \Delta\dot{x}_b \end{bmatrix}, \qquad \dot{\mathbf{x}} = \begin{bmatrix} \Delta\dot{\theta} \\ \Delta\ddot{\theta} \\ \Delta\dot{P}_a \\ \Delta\dot{P}_b \\ \Delta\dot{x}_a \\ \Delta\ddot{x}_a \\ \Delta\dot{x}_b \\ \Delta\ddot{x}_b \end{bmatrix}, \qquad \mathbf{i}^* = \Delta i.$$

Based on this state space model, the frequency response analysis has been conducted for all the output parameters denoted in the matrix as represented in Figs 6a–6e with the help of MatLAB. It can be observed from Figs 6a, 6d, and 6e that the supply pressure of the system does not influence the torque motor dynamics and spool displacement dynamics.

Figures 6b and 6c show that variation in the supply pressure affects the chamber pressure dynamics. It can be observed that a neck is formed in pressure gain

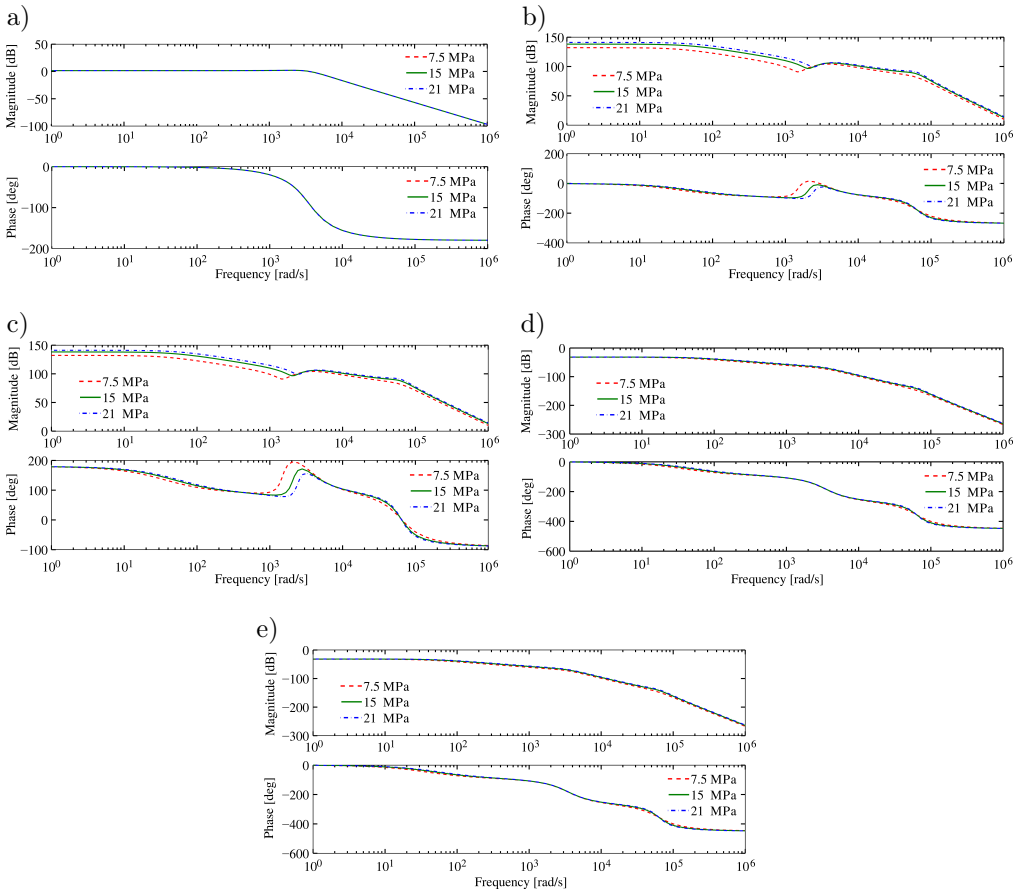

FIG. 6. Frequency response of the system: a) torque motor, θ, b) chamber pressure, P_a, c) chamber pressure, P_b, d) displacement of spool 1, x_a, e) displacement of spool 2, x_b.

characteristics of the system near the frequency 3.2e03 rad/s approximately, for the present set of parameters. The corresponding phase characteristics also show a sudden jump at this frequency.This may be due to pressure feedback used in the two-spool servovalve under consideration, instead of 'force feedback' used in conventional two-stage servovalve. It is also clear from the result that the magnitude of the jump and neck decreases with an increase in magnitude of supply pressure.It is to be noted that standalone hydraulic systems operate in lower frequency ranges for which there is no substantial effect on the system as observed from Figs 6b and 6c. However, modern high performance servocontrol systems utilize a combination of low operation frequency. Hydraulic components with Electrical and Electronic components having higher operational frequency. This may lead to such instances of sudden fluctuations in the chamber pressure dynamics which the servovalve designer must take into consideration.

7. Conclusions

This paper establishes a pressure feedback model of a non-conventional electrohydraulic servovalve by means of a dimensional linearization process for a set of nonlinear equations describing the dynamics of the servovalve. The model takes into account the flow forces on the spool in the axial direction and the compressible nature of the working fluid. The linear model is coded in the MATLAB/Simulink environment to study the dynamic performance of the valve against step input in current at the torque motor end. The frequency response is analysed through state-space model by applying various supply pressures on the system.

On the basis of the mathematical analysis of the system, it can be asserted that the design changes at any condition can be analysed very promptly. The dynamic model of the system will also be helpful in designing and analysis of the control system. The frequency analysis of the state space model reveals that the system operation at high frequency bands is not recommendable owing to the sensitive interfacing between the electrical and hydraulic components which is quite evident in chamber pressure dynamics.

Acknowledgements

The authors acknowledge the support provided by the members of Mechanical systems and Control Laboratory of Jadavpur University, especially Mr. Shouvik Chaudhuri for ensuing technical discussion regarding the present work.

Declaration of conflicting interests

The author(s) declared no potential conflicts of interest with respect to the research, authorship and/or publication of this article.

Funding

The author(s) received no financial support for the research, authorship and/or publication of this article.

References

1. Tsai S.T., Akers A., Lin S.J., *Modeling and dynamic evaluation of a two-stage two-spool servovalve used for pressure control*, Journal of Dynamic Systems, Measurement and Control, **113**(4): 709–713, 1991.

2. Merritt H.E., *Hydraulic control systems*, Wiley, New York, pp. 147–150 and 312–318, 1967.

3. El-Araby M., El-Kafrawy A., Fahmy A., *Dynamic performance of a nonlinear non-dimensional two stage electrohydraulic servovalve model*, International Journal of Mechanics and Materials in Design, **7**(2): 99–110, 2011.

4. Li P.Y., *Dynamic redesign of a flow control servovalve using a pressure control pilot*, Journal of Dynamic Systems, Measurement and Control, **124**(3): 428–434, 2002.

5. Singaperumal M., Hiremath S.S., Krishnakumar R., *Frequency response of critical components of a hydraulic servovalve*, Proceedings 11th National Conference on Machines and Mechanics, pp. 319.

6. Anderson R.T., Li P.Y., *Mathematical modeling of a two spool flow control servovalve using a pressure control pilot*, Journal of Dynamic Systems, Measurement and Control, **124**(3): 420–427, 2002.

7. Kim D.H., Tsao T.C., *A linearized electrohydraulic servovalve model for valve dynamics sensitivity analysis and control system design*, Journal of Dynamic Systems, Measurement and Control, **122**(1): 179–187, 2000.

8. Lin S.J., Akers A., *A dynamic model of the flapper-nozzle component of an electro-hydraulic servovalve*, Journal of Dynamic Systems, Measurement and Control, **111**(1): 105–109, 1989.

9. Bang Y.B., Joo C.S., Lee K.I., Hur J.W., Lim W.K., *Development of a two-stage high speed electrohydraulic servovalve systems using stack-type piezoelectric elements*, Proceedings of the IEEE/ASME International Conference on Advanced Intelligent Mechatronics, **1**, pp. 131–136, 2003, July.

10. Jie Y., Hongliang P., *Effects of supply pressures on two-stage electro-hydraulic servo valve*, Advances in Biomedical Engineering, **11**: 33, 2012.

11. Yuan Q.H., Jae Y.L., *Modeling and control of two stage twin spool servo-valve for energy-saving*, Proceedings of the 2005, American Control Conference, IEEE, pp. 4363–4368, 2005.

12. Yoshida F., Miyakawa S., *Effect of parameters on frequency characteristics of proportional control valve using tap water*, Proceedings of the 8th JFPS International Symposium on Fluid Power, Okinawa, Japan, 2011.

13. Gordić D., Babić M., Jovičić N., *Modelling of spool position feedback servovalves*, International Journal of Fluid Power, **5**(1): 37–51, 2004.

14. Yuan Q., Li P.Y., *Using steady flow force for unstable valve design: modeling and experiments*, Journal of Dynamic Systems, Measurement and Control, **127**(3): 451–462, 2005.

15. Manring N.D., Zhang S., *Pressure transient flow forces for hydraulic spool valves*, Journal of Dynamic Systems, Measurement and Control, **134**(3): 034501, 2012.

16. Mondal N., Datta B.N., *A study on electro hydraulic servovalve controlled by a two spool valve*, International Journal of Emerging Technology and Advanced Engineering, **23**(3): 479–484, 2013.

17. Ogata K., *Modern control engineering*, 5th ed., Prentice Hall, pp. 666–672, 1970.

18. Yuan Q., Lew J.Y., *Modeling and control of two stage twin spool servo-valve for energy-saving*, Proceedings of the American Control Conference, IEEE, pp. 4363–4368, 2005.

Received July 24, 2018; accepted version February 28, 2019.
